Plastocyanin−Cytochrome *f* Interactions: The Influence of Hydrophobic Patch Mutations Studied by NMR Spectroscopy†

Peter B. Crowley,‡ Nadejda Vintonenko,§ George S. Bullerjahn,§ and Marcellus Ubbink*,‡

Leiden Institute of Chemistry, Leiden University, Gorlaeus Laboratories, P.O. Box 9502, 2300 RA Leiden, The Netherlands, and Center for Photochemical Sciences, Department of Biological Sciences, Bowling Green State University, Bowling Green, Ohio 43403-0212

Received June 25, 2002; Revised Manuscript Received November 7, 2002

ABSTRACT: Transient complex formation between plastocyanin from *Prochlorothrix hollandica* and cytochrome *f* from *Phormidium laminosum* was investigated using nuclear magnetic resonance (NMR) spectroscopy. Binding curves derived from NMR titrations at 10 mM ionic strength reveal a 1:1 stoichiometry and a binding constant of 6 (±2) × 10^3 M^{-1} for complex formation, 1 order of magnitude larger than that for the physiological plastocyanin-cytochrome *f* complex from *Ph. laminosum*. Chemical-shift perturbation mapping indicates that the hydrophobic patch of plastocyanin is involved in the complex interface. When the unusual hydrophobic patch residues of *P. hollandica* plastocyanin were reverted to the conserved residues found in most other plastocyanins (Y12G/P14L), the binding constant for the interaction with cytochrome *f* was unaffected. However, the chemical shift perturbation map was considerably different, and the size of the average perturbation decreased by 40%. The complexes of both the wild-type and double mutant plastocyanin with cytochrome *f* were sensitive to ionic strength, contrary to the physiological complex. The possible implications of these findings for the mechanism of transient complex formation are discussed.

Energy transducing membranes couple electron transport along the membrane to proton translocation across the membrane, thereby generating an electrochemical gradient, which drives the formation of ATP (*1*). The electron-transfer chains involved in such processes as photosynthesis and respiration, consist of both membrane-bound complexes and mobile electron carriers. To maintain high turnover conditions, the interactions of the membrane-bound and the mobile components of the chain proceed via transient complex formation (*2*). Such complexes are characterized by low binding affinities, on the order of μM^{-1}−mM^{-1}, and short lifetimes on the millisecond time scale. While the interactions of the redox partners are tuned to be of low affinity, the specificity should be such that electron transfer can occur efficiently. In general, redox proteins must participate in transient interactions with various different partner proteins in the cell. Therefore, the protein surface must necessarily recognize and interact with partners, which have distinct surface properties and structures. This gives rise to the question of whether highly stereospecific complexes can be formed (*3*, *4*).

During photosynthesis, the type I copper protein, plastocyanin (Pc), transports electrons between the membrane-bound cytochrome *bf* (cyt*bf*)[1] complex and photosystem I (PSI) (*5*, *6*). Two structures of the transient complex formed between Pc and cytochrome *f* (cyt*f*), a soluble component of the cyt*bf* complex (*7*, *8*), have been solved previously (*9*, *10*). It was found that complementary charged surfaces as well as hydrophobic patches contribute to the complex interface formed between turnip cyt*f* and spinach Pc (*9*). In contrast, the complex from the thermophilic cyanobacterium *Phormidium laminosum* (Figure 1) relies primarily on hydrophobic interactions (*10*). Similarly, it has been shown by in vitro kinetic studies that the rate of electron transfer between the plant proteins has a strong ionic strength dependence while association of the cyanobacterial proteins is only weakly affected by salt (*11*−*13*). The evidence suggests, therefore, that distinct mechanisms of photosynthetic electron transport have evolved in different organisms.

The "north end" of the Pc molecule is composed of about 25 residues, which surround the exposed histidine ligand of the copper site (*14*, *15*). A sequence alignment (*16*) of the known Pc sequences reveals that, with the exception of Pc from the fern *Dryopteris crassirhizoma* (*17*), 16 of these "north end" residues are conservatively hydrophobic. The structure of the north end differs significantly between the eukaryotic and cyanobacterial variants of Pc. Long chain aliphatic residues, such as Leu and Met, are more common in cyanobacterial Pc, resulting in a more extensive hydrophobic patch (*18*). This region of the protein surface was shown to be crucial for the interactions of Pc and cyt*f* (*9*,

† Financial support for G.S.B. was provided by Grants 9634049 and 0070334 from the National Science Foundation.

* To whom correspondence may be addressed. Email: m.ubbink@chem.leidenuniv.nl. Telephone: +31 71 527 4628.

‡ Leiden University.

§ Bowling Green State University.

[1] Abbreviations: Pc, plastocyanin; cyt*f*, cytochrome *f*; cyt*bf*, cytochrome *bf*; PSI, photosystem I; NMR, nuclear magnetic resonance; HSQC, heteronuclear single quantum coherence spectroscopy; NOESY, nuclear Overhauser enhancement spectroscopy; TOCSY, total correlation spectroscopy; 1D, one-dimensional.

10.1021/bi026349b CCC: $22.00
Published on Web 12/07/2002

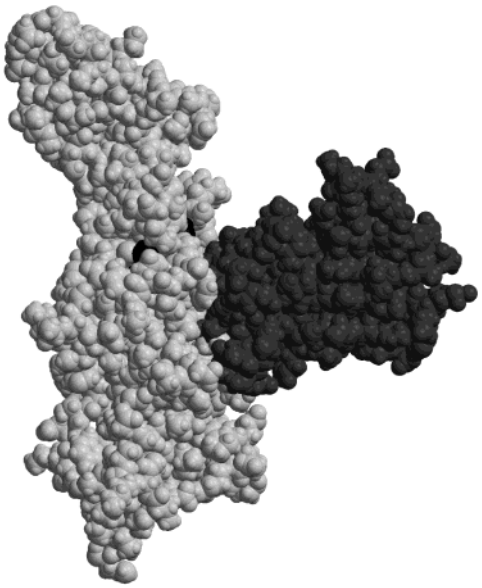

FIGURE 1: Space filling model of the complex formed between Pc (*47*) (dark gray) and cyt*f* (*48*) (light gray, heme in black) from *Ph. laminosum* (*10*). The complex interface is composed of patches of hydrophobic residues surrounding the redox centers on both proteins. The figure was drawn using Molscript (*49*) and rendered in Raster3D (*50*).

10). It has also been shown that the reactivity of plant Pc can be affected by hydrophobic patch mutants. While the binding affinity of spinach Pc for cyt*f* decreased upon mutation of Leu12 to Ala (*19*), replacement of Gly10 by the bulkier side-chains of Val, Leu, and Met resulted in increased second-order rate constants for the reduction by cyt*bf* particles (*20*). In contrast, the electron-transfer rate for the reduction of PSI was decreased in the mutants, Gly10Leu (*21*) and Leu12Ala (*22*).

Pc from the cyanobacterium, *Prochlorothrix hollandica* is unusual in that residues 12 and 14 are Tyr and Pro respectively (*23*, *24*). Gly and Leu occupy these positions in all other Pc sequences, with the exception of fern Pc, which has a Phe at the position corresponding to Leu14 (*17*). Pc's from *P. hollandica* and *Ph. laminosum* share 47% sequence identity. When only the north end residues are considered the sequence conservation increases to 61%. To assess the contribution of residues Tyr12 and Pro14 to protein−protein interactions, the complex of *P. hollandica* Pc and *Ph. laminosum* cyt*f* was studied using NMR spectroscopy. The results indicate that *P. hollandica* Pc and cyt*f* form a 1:1 complex with a binding site which involves the hydrophobic patch on Pc. Despite the large changes introduced in the binding site by the double mutation of Y12G/P14L, the binding affinity for cyt*f* was not significantly affected. However, a large decrease in the average chemical shift perturbation was observed for the mutant compared to the wild-type *P. hollandica* Pc. These results provide new insights into the nature of the binding sites found in transient protein complexes.

MATERIALS AND METHODS

Protein Preparation. ^{15}N-labeled *Ph. laminosum* Pc and unlabeled cyt*f* were prepared as described previously (*10*, *25*). Mutant and wild-type ^{15}N-labeled *P. hollandica* Pc were expressed as inclusion bodies in *Escherichia coli* BL21(DE3) pLysS (Novagen, Madison, WI) as previously described (*23*), with the exception that the expression medium was M9 glucose (*26*) containing 1 g/L $^{15}NH_4Cl$. Specifically, the *P. hollandica* Pc expression plasmid pVAPC10 (*23*) was used as a template for both PCR-mediated mutagenesis (Stratagene QuikChange kit, La Jolla, CA) and T7 RNA polymerase-dependent expression. The construction of the double mutant Y12G/P14L by mutagenic PCR has been reported previously (*27*). Reconstitution of the inclusion bodies was performed using a modified, high-yield method. Inclusion bodies from a 1 L culture were harvested and dissolved in 10 mL of 0.2 M Tris (pH 8.5), 6 M guanidine−HCl. β-Mercaptoethanol was added to 50 mM and the pH adjusted to 7.0. The resulting solution was diluted with buffer containing copper (0.2 M Tris, pH 7.0, 1 mM $CuCl_2$, 25 mM β-mercaptoethanol) to a final concentration of 1.5 M guanidine−HCl. Following two dialysis steps against the copper containing buffer and one dialysis step in the same buffer lacking copper, the protein was concentrated by reverse dialysis and filtration (Centricon, Amicon Corp., Beverly MA). Refolded Pc preparations were analyzed by absorption and far-UV circular dichroism spectroscopy as described previously (*23*). Typically, yields of 20 mg/L culture were obtained with an A_{280}/A_{602} ratio of 2.8−3.1.

NMR Samples. Pc protein solutions were concentrated by ultrafiltration (Amicon, YM5 membrane) and exchanged into 10 mM potassium phosphate pH 6.0, 10% D_2O, 1.0 mM sodium ascorbate. For the assignment of both *P. hollandica* Pc and Pc Y12G/P14L, 4.0 mM ^{15}N-labeled samples were prepared. The protein concentrations were determined by optical spectroscopy using an ϵ_{602} of 4.9 mM^{-1} cm^{-1} for the oxidized protein. Cyt*f* samples were prepared in the same buffer and concentrated using Millipore Ultrafree centrifugal tubes with a 5 kDa molecular weight cutoff. The protein concentration was determined using an ϵ_{556} of 31.5 mM^{-1} cm^{-1} for the ferrous form. To investigate protonation of His85 in *P. hollandica* Pc and Pc Y12G/P14L, pH titrations were performed on 2.0 mM samples. The pH was adjusted by the addition of microliter aliquots of 1 M NaOH or 1 M HCl, and 1D ^{1}H NMR spectra were acquired over the range pH 4.5−7.8. To determine a binding constant for the complex of *Ph. laminosum* Pc and cyt*f*, an NMR titration was performed in which a 0.33 mM ^{15}N-Pc sample was titrated with microliter aliquots of a 1.83 mM cyt*f* stock. Complex formation between *P. hollandica* Pc and *Ph. laminosum* cyt*f* was investigated by titrating microliter aliquots of a 2.54 mM cyt*f* stock solution into a 0.41 mM ^{15}N-Pc. To investigate complex formation with the double mutant a similar NMR titration was performed using a 0.38 mM sample of ^{15}N-Pc Y12G/P14L and a 2.86 mM cyt*f* stock. After each addition of protein, the sample pH was verified, and ^{1}H-^{15}N HSQC spectra were recorded. Ionic strength effects on complex formation were investigated by the addition of 50, 100, and 200 mM NaCl to samples containing 2:1 mixtures of *Ph. laminosum* cyt*f* and either *P. hollandica* Pc or Pc Y12G/P14L.

NMR Spectroscopy. All spectra were acquired at 300 K on a Bruker DMX 600 NMR spectrometer. For sequence-specific assignment of the backbone resonances of *P. hollandica* Pc and Pc Y12G/P14L, 2D ^{1}H-^{15}N HSQC (*28*), 2D ^{1}H-^{15}N HSQC−NOESY, and 2D ^{1}H-^{15}N HSQC-TOCSY spectra were recorded. XWINNMR was used for spectral

processing and the assignments were performed in XEASY (*29*). For measurements on the complexes, ^{1}H-^{15}N HSQC spectra were recorded with spectral widths of 40.0 ppm (^{15}N) and 16.0 ppm (^{1}H). Analysis of the chemical-shift perturbation ($\Delta\delta_{Bind}$) with respect to the free protein assignments was performed in XEASY.

Titration Curves. Binding curves were obtained by plotting $\Delta\delta_{Bind}$ against the molar ratio (R) of [cyt*f*]:[Pc]. The data were fit (nonlinear least squares) to a one-site binding model (*11*), which explicitly treats the total concentration of both proteins, with *R* and $|\Delta\delta_{Bind}|$ as the independent and dependent variables, respectively, and the maximum chemical-shift change ($\Delta\delta_{Max}$) and the binding constant (K_a) as the fitted parameters. A global fit of the data was performed in which the curves were fitted simultaneously to a single K_a value, while $\Delta\delta_{Max}$ was allowed to vary for each resonance.

Chemical-Shift Mapping. The percentage of bound protein was calculated from the ratio of the experimentally observed $|\Delta\delta_{Bind}|$ and the fitted $\Delta\delta_{Max}$, for the seven most strongly shifted residues in the complexes of cyt*f* with *P. hollandica* Pc and Pc Y12G/P14L. The shifts observed in the complex with 2.1 equiv of cyt*f* were then extrapolated to 100% bound for all residues. The average chemical-shift perturbation ($\Delta\delta_{Avg}$) of each amide was calculated using eq 1 (*30*)

$$\Delta\delta_{Avg} = \sqrt{\frac{(\Delta\delta N/5)^2 + \Delta\delta H^2}{2}} \quad (1)$$

where $\Delta\delta N$ is the change in the ^{15}N chemical-shift and $\Delta\delta H$ is the change in the $^1H^N$ chemical-shift when the protein is 100% bound to cyt*f*. $\Delta\delta_{Avg}$ versus the residue number was plotted for both complexes and the shifts were categorized as follows: insignificant, <0.025 ppm; small, <0.100 ppm; medium, <0.175 ppm; and large, <0.350 ppm. Chemical-shift maps were prepared in Grasp (*31*) by coloring surface representations of *P. hollandica* Pc (*24*) and Pc Y12G/P14L according to their calculated $\Delta\delta_{Avg}$. The structure of Pc Y12G/P14L has not been determined, so a model was built in Swiss-MODEL (*32*) using the NMR structure of *P. hollandica* Pc (*24*) as a template.

RESULTS

Assignment of P. hollandica Pc and Pc Y12G/P14L. A complete homonuclear assignment has been reported previously for *P. hollandica* Pc (*24*). All 88 observable backbone amides were resolved in the ^{1}H-^{15}N HSQC spectrum. Sequence-specific assignment of the amide resonances was achieved by comparison of the homonuclear assignments with 2D ^{1}H-^{15}N HSQC-TOCSY and HSQC−NOESY spectra. A similar approach was taken for the assignment of the double mutant Pc Y12G/P14L. Compared with those in the wild-type Pc, large chemical-shift changes occur in the ^{1}H-^{15}N HSQC spectrum of Pc Y12G/P14L. A difference plot between the averaged $^1H^N$ and ^{15}N resonance assignments of *P. hollandica* Pc and Pc Y12G/P14L ($\Delta\delta_{Mut}$), illustrates the regions of the protein which are affected by the double mutation (Figure 2). Four stretches of the primary structure, which contribute to the hydrophobic patch, experience significant chemical-shift changes in the mutant. As expected, the largest effects are observed in the immediate vicinity of the mutations. In particular, large shifts are observed for

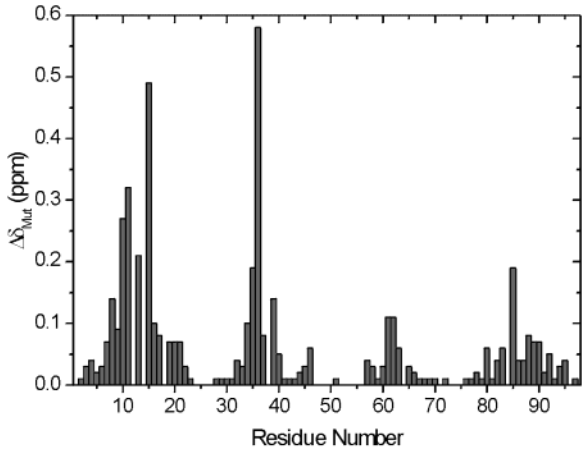

FIGURE 2: Difference plot between the averaged ^{1}H and ^{15}N resonance assignments of *P. hollandica* Pc and Pc Y12G/P14L ($\Delta\delta_{Mut}$) vs residue number, illustrating the regions of the protein which are affected by the double mutation.

Lys11 and Leu15, which neighbor residues 12 and 14, respectively. Val36, the side chain of which makes van der Waals contact with both Tyr12 and Pro14, experiences the largest change arising from the mutations. It is probable that the shifts reflect subtle structural rearrangements of the hydrophobic patch. In all of the 19 NMR structures of *P. hollandica* Pc the side-chain of Tyr12 is highly solvent exposed and projects outward from the hydrophobic patch (*24*). The nearest amide group, Val36, is more than 5.5 Å from the aromatic ring (*24*). Therefore, ring current effects are not expected to make a large contribution to the difference in the amide resonance assignments. The large $\Delta\delta_{Mut}$ of Val36 is more likely caused by the proximity of its side chain to both Tyr12 and Pro14. A notable similarity was observed for the assignments of Gly12 and Leu14 in the double mutant and in *Ph. laminosum* Pc (*10*). In fact, the $^1H^N$ chemical shift of 16 conserved north end residues found in both proteins were within 0.3 ppm of each other, indicating that the structure of the hydrophobic patch is homologous (*33*).

Protonation of His85 in P. hollandica Pc and Pc Y12G/P14L. The exposed His ligand of reduced Pc can dissociate from the cuprous ion to become protonated at low pH (*34*−*37*). In the NMR structure of *P. hollandica* Pc, the side chain of Pro14 makes van der Waals contact with the imidazole ring of His85. Therefore, the mutation Pro14Leu is likely to influence the conformation of the imidazole ring, which may in turn affect the pK_a of this residue. This suggestion is supported by the fact that His85 experiences a large chemical-shift change in the double mutant (Figure 2). Fern Pc, which has a Phe in place of the semiconserved Leu, does not exhibit a protonation of the His ligand (*17*, *38*). Recently, it was shown that the chemical shift perturbation ($\Delta\delta_{Bind}$) observed for Pc in the presence of cyt*f* is dependent on the protonation state of the His ligand (*10*). For these reasons the pH behavior of wild-type and double mutant *P. hollandica* Pc, was investigated by NMR spectroscopy. To determine the pK_a of His85, the chemical shift of the $^1H^{\epsilon 2}$ resonance of His39 was followed as a function of pH. It has previously been shown for *Ph. laminosum* Pc that this nucleus as well as many of the backbone amides of north end residues are useful probes of pH effects in the active

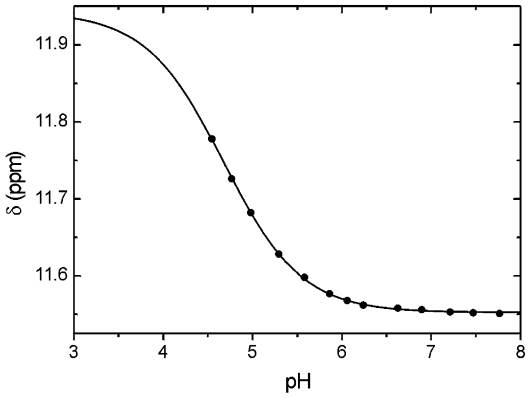

FIGURE 3: Chemical-shift of the $^1H^{\epsilon 2}$ resonance of His39 as a function of pH. 1D ^1H NMR spectra of *P. hollandica* Pc were recorded over the range of pH 4.5−7.8. The data were fitted (nonlinear least squares) to the equation $\delta = (K_a\delta_H + [H^+]\delta_L)/(K_a + [H^+])$, where δ_H and δ_L represent the chemical shifts at high and low pH respectively, yielding a pK_a value of 4.7 (±0.1) at 10 mM ionic strength, 300 K.

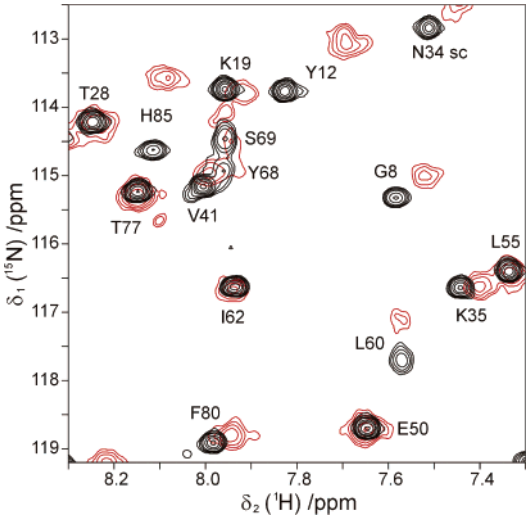

FIGURE 4: Spectral region from the overlaid ^1H-^{15}N HSQC spectra of free *P. hollandica* Pc (black) and *P. hollandica* Pc in the presence of 2.1 equiv of *Ph. laminosum* cyt*f* (red).

site (*39*). The titration curves of 27 backbone amide nuclei in *Ph. laminosum* Pc yielded identical pK_a values for protonation of the histidine ligand (*39*). The pK_a of His85 in *P. hollandica* Pc was determined to be 4.7 ± 0.1 for the wild-type (Figure 3) and 4.5 ± 0.1 for the double mutant (data not shown). Therefore Pro14 does not strongly influence the pK_a of His85 and the $\Delta\delta_{Mut}$ observed at pH 6.0 is not related to His85 protonation. It can be concluded furthermore that the $\Delta\delta_{Bind}$ experienced by the wild-type and mutant protein in complex with cyt*f* at pH 6.0 will not be affected by protonation of His85.

The Complex of P. hollandica Pc and Ph. laminosum Cyt f. The presence of cyt*f* gave rise to distinct changes in the ^1H-^{15}N HSQC spectrum of *P. hollandica* Pc (Figure 4). Forty-six backbone amides experienced an $|\Delta\delta_{Bind}| \geq 0.02$ ppm ^1H and/or ≥ 0.10 ppm ^{15}N (Table S1). In addition to chemical-shift perturbation, a general broadening of the amide resonances was observed (Figure 5A), as expected for complex formation (*40*). The extent of chemical-shift perturbation and line broadening increased with the addition of increasing amounts of cyt*f*. A single, averaged resonance

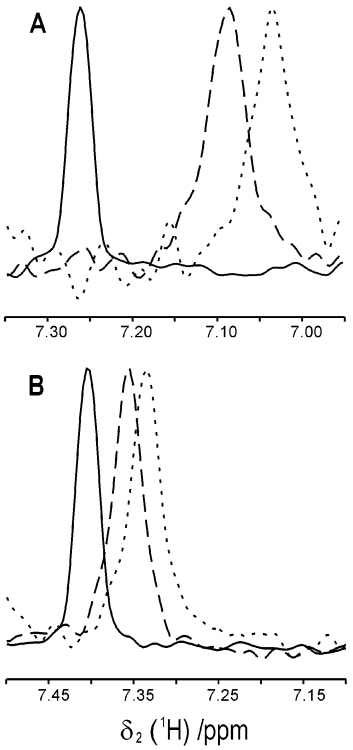

FIGURE 5: Cross-sections along the F_2 dimension through the $^1H^N$ resonance of Leu15 in (A) *P. hollandica* Pc and (B) Pc Y12G/P14L. The resonance of the free protein is shown as a solid line. In the presence of 1.1 equiv of cyt*f* the resonance is both broadened and shifted (dashed line). The resonance at 2.1 equiv of cyt*f* is shown as a dotted line.

was detected for each amide, indicating that the free and bound forms of Pc were in fast exchange on the NMR time scale (*40*). Side-chain amides were also affected upon complex formation. The intensity of the resonances of Asn34 and Asn40 decreased, and a shift of −0.15 ppm was observed for the $^{15}N^{\delta}$ of Asn34. Such broadening was also observed for Asn34 and Asn40 of *Ph. laminosum* Pc in complex with cyt*f* (*10*).

Binding curves for the interaction of *P. hollandica* Pc and *Ph. laminosum* cyt*f* were obtained by plotting $\Delta\delta_{Bind}$ against the molar ratio of [cyt*f*]:[Pc] for the most strongly affected resonances (Figure 6). Saturation of the chemical-shift changes was not observed, suggesting a moderately low binding affinity. A global fit of the curves to a 1:1 binding model (*11*) yielded a binding constant of 6 (±2) × 10^3 M^{-1}, approximately 20 times higher than the binding constant for the physiological partner *Ph. laminosum* Pc (Figure 6) (*10*). The experimental $|\Delta\delta_{Bind}|$ (observed in the presence of 2.1 equiv of cyt*f*) and the fitted $\Delta\delta_{Max}$ are shown in Table 1. From the ratio of $|\Delta\delta_{Bind}|$ and $\Delta\delta_{Max}$ it was calculated that 70% of Pc was bound in the presence of 2.1 molar equiv of cyt*f*. The shifts experienced by all of the backbone amide nuclei in Pc were extrapolated to 100% bound and the $\Delta\delta_{Avg}$ was plotted in Figure 7. The affected nuclei occur in four distinct regions of the primary structure, residues 6−19, 34−42, 56−70, and 80−92. These regions of the primary structure contain the four loops, which make up the north end of the β-sandwich structure of Pc (*15*, *24*). Of the 40 residues, which experienced a significant $\Delta\delta_{Avg}$, 23 were hydrophobic, nine were polar, and eight were charged residues. The largest effects were found for Tyr12, Ala13,

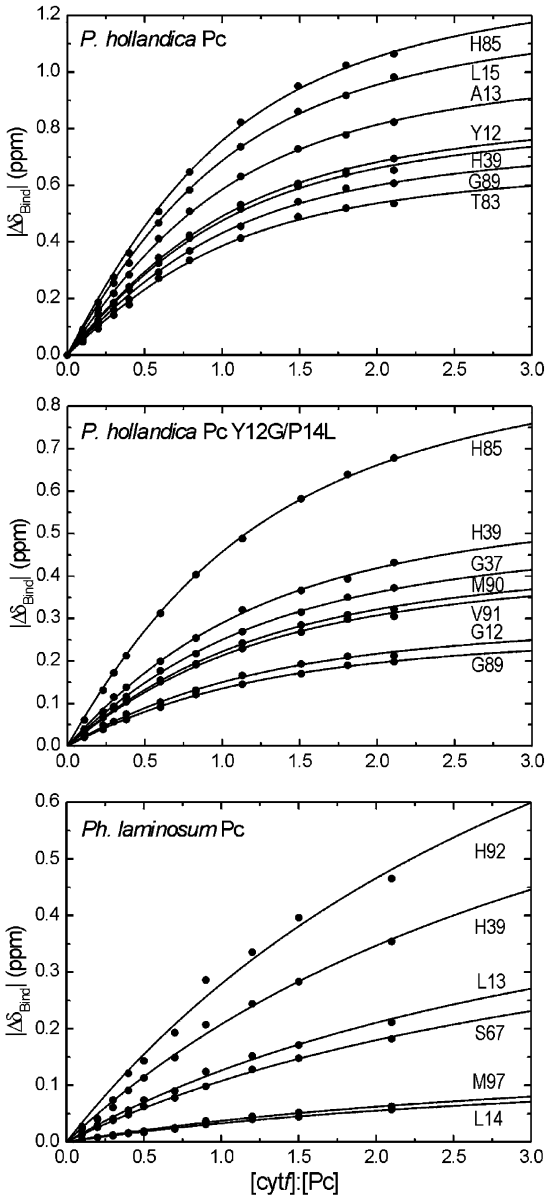

FIGURE 6: Titration curves for complex formation between Pc and cyt*f*. $|\Delta\delta_{Bind}|$ of the indicated residues are plotted against the molar ratio of cyt*f* to Pc. The solid lines represent nonlinear least-squares fits to a 1:1 binding model (*11*), yielding binding constants of 6 (± 2) $\times 10^3$, 4 (± 2) $\times 10^3$, and $\sim 0.3 \times 10^3$ M^{-1} for the complexes of *Ph. laminosum* cyt*f* with *P. hollandica* Pc, Pc Y12G/P14L, and *Ph. laminosum* Pc, respectively.

Leu15, and His85. Chemical-shift perturbation mapping reveals that the affected residues are localized on one end of *P. hollandica* Pc (Figure 8A), which results in a well-defined binding site surrounding the exposed histidine ligand (His85) of the copper. The importance of the hydrophobic patch of Pc for complex formation with cyt*f* is therefore clearly illustrated.

The complex of *P. hollandica* Pc and *Ph. laminosum* cyt*f* was also investigated at 50, 100, and 200 mM NaCl. The salt dependence of the most strongly shifted resonances in the complex was plotted in Figure 9. As the ionic strength was increased, the observed $\Delta\delta_{Bind}$ decreased. At 200 mM NaCl the $\Delta\delta_{Bind}$ was on average 35% lower compared with the "zero salt" experiment, indicating that attractive electrostatic interactions play a role in complex formation.

Table 1: Determination of the Percentage Bound *P. hollandica* Pc in Complex with *Ph. laminosum* Cyt*f*

residue	$\lvert\Delta\delta_{Bind}\rvert$[a] (ppm)	$\Delta\delta_{Max}$[b] (ppm)	% bound
Y12	0.69	0.98	71
A13	0.82	1.17	70
L15	0.98	1.38	71
H39	0.65	0.95	69
T83	0.54	0.77	69
H85	1.06	1.51	70
G89	0.61	0.86	71

[a] Observed in the presence of 2.1 equiv of *Ph. laminosum* cyt*f*. [b] The fitted $\Delta\delta_{Max}$ (see Materials and Methods, Figure 6) corresponds to the chemical-shift perturbation when Pc is 100% bound in the complex with cyt*f*.

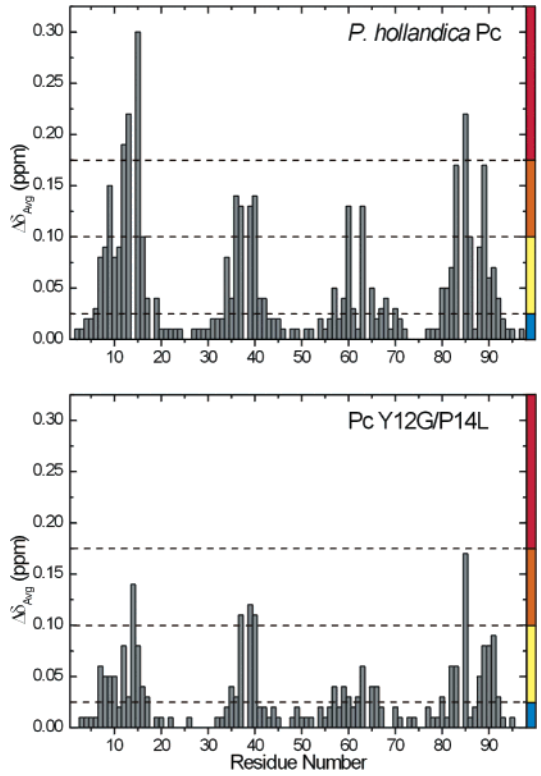

FIGURE 7: Average chemical-shift perturbation ($\Delta\delta_{Avg}$), extrapolated to 100% bound, experienced by *P. hollandica* Pc and Pc Y12G/P14L in complex with *Ph. laminosum* cyt*f*. The color bars indicate the $\Delta\delta_{Avg}$ categories: large (red), medium (orange), small (yellow), and insignificant (blue), for chemical-shift mapping onto surface representations of the two proteins (Figure 8).

The Complex of P. hollandica Pc Y12G/P14L and Cytf. Changes in the ^{1}H-^{15}N HSQC spectrum of Pc Y12G/P14L resulting from the addition of cyt*f* were comparable to the changes observed with the wild-type protein. In the presence of 2.1 equiv of cyt*f*, 37 backbone amides of the double mutant experienced $|\Delta\delta_{Bind}| \geq 0.02$ ppm ^{1}H and/or ≥ 0.10 ppm ^{15}N (Table S1). Although similar nuclei were affected, the magnitude of the observed shifts was diminished with respect to the shifts in the complex with the wild-type protein. Binding curves for the complex of Pc Y12G/P14L and cyt*f* were fit to a binding constant of 4 (± 2) $\times 10^3$ M^{-1} (Figure 6). Within error, the binding curves for the wild-type and mutant *P. hollandica* Pc could be fitted to identical K_a values. Despite the similar binding affinity, the extent of line broadening was lower in the mutant complex. The chemical

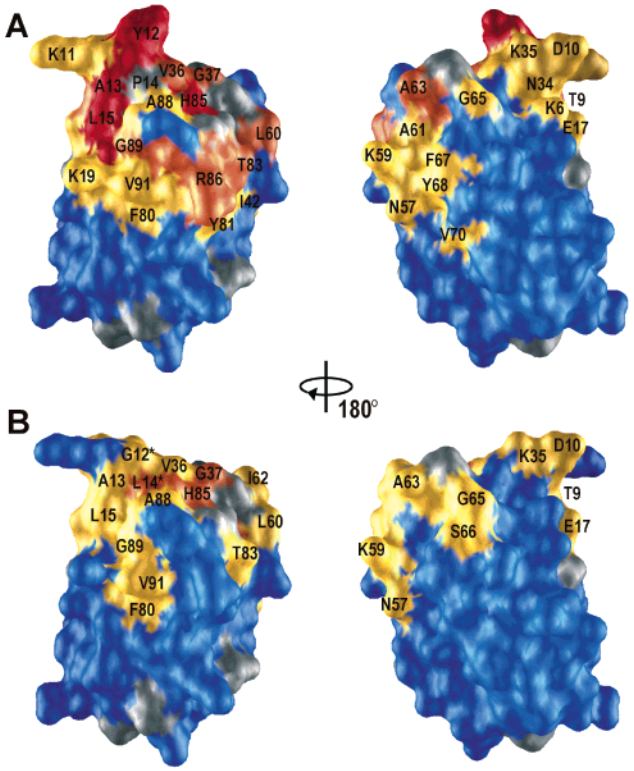

FIGURE 8: Chemical-shift mapping of (A) *P. hollandica* Pc and (B) Pc Y12G/P14L, in the presence of *Ph. laminosum* cyt*f*. Residues are colored according to the categories in Figure 7. Prolines are colored gray. The mutated residues are indicated with an asterix.

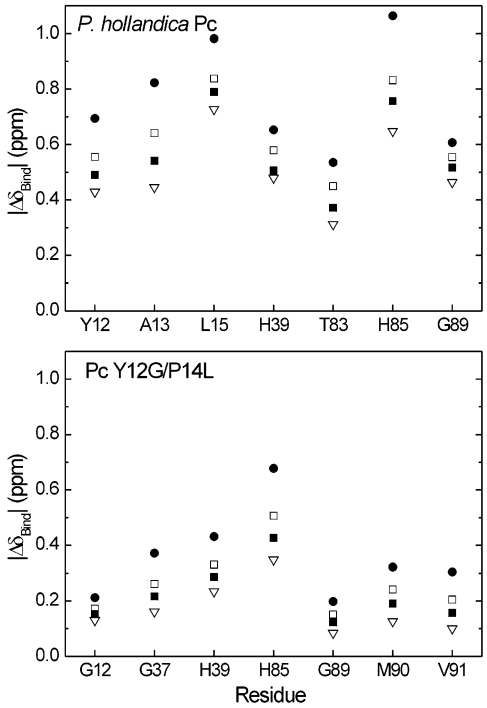

FIGURE 9: Salt dependence of $|\Delta\delta_{Bind}|$ for the most strongly shifted residues, observed in the complexes of *Ph. laminosum* cyt*f* with *P. hollandica* Pc and Pc Y12G/P14L, at (●) 0, (□) 50, (■) 100, and (▽) 200 mM NaCl.

shift and the line width at half-height of Leu15 of *P. hollandica* Pc and Pc Y12G/P14L in complex with cyt*f* are compared in Figure 5. At 2.1 equiv of cyt*f* the $^1H^N$ resonance of Leu15 is broadened by ~16 Hz in the wild-type protein and by ~10 Hz in Pc Y12G/P14L. The line broadening was on average 4 Hz lower for the complex with the mutant protein. This disparity in line broadening effects is also evidenced by the significant difference in the signal-to-noise ratio between the wild-type and mutant complexes (Figure 5). The differences in the line broadening were the same for shifted and nonshifted resonances and thus cannot be caused by exchange effects. They could however, reflect a difference in rotational correlation time of Pc in the complex with cyt*f* (see below).

From the ratio of $|\Delta\delta_{Bind}|$ and $\Delta\delta_{Max}$, it was calculated that 62% of Pc Y12G/P14L was bound in the presence of 2.1 equiv of cyt*f*. The observed chemical-shift perturbation was extrapolated to 100% bound, and the $\Delta\delta_{Avg}$ for each backbone amide was plotted in Figure 7. The affected nuclei are found in the same four regions of the primary structure as for the wild-type protein. Of the 31 residues, which experienced a significant $\Delta\delta_{Avg}$, 21 were hydrophobic, six were polar, and four were charged. The largest effects were found for Leu14, Gly37, His39, Asn40, and His85. As expected, the chemical-shift map indicates that the hydrophobic patch of Pc Y12G/P14L is involved in complex formation (Figure 8B). From Figures 7 and 8, it is evident, however, that there are large differences in the binding effects on both proteins. Although a similar region of the protein is affected, the binding site is less extensive for the double mutant. Compared with the wild-type protein, $\Delta\delta_{Avg}$ was on average 40% lower for Pc Y12G/P14L (Figure 7). Notable exceptions include Lys35/Lys59, which experience the same $\Delta\delta_{Avg}$ in both complexes, Met90/Val91, which have a 30% increased $\Delta\delta_{Avg}$, and Ala13/Arg86, which have a 90% decreased $\Delta\delta_{Avg}$ in the mutant protein.

The salt dependence of the most strongly shifted resonances in the complex of Pc Y12G/P14L and cyt*f* was plotted in Figure 9. As was the case for the wild-type protein, the observed $\Delta\delta_{Bind}$ decreased with increasing ionic strength. At 200 mM NaCl the $\Delta\delta_{Bind}$ was decreased by 55% on average, indicating that the binding constant was considerably reduced. Complex formation with the double mutant appears, therefore, somewhat more susceptible to ionic strength effects than the wild-type protein (Figure 9), suggesting that the balance of hydrophobic and electrostatic interactions has been altered by the mutations.

It is noteworthy that the amide resonances of His85 and Leu14 in Pc Y12G/P14L shift in the same way (a large negative ^{15}N shift for His and a large negative $^1H^N$ shift for Leu, Table S1) as the corresponding residues, His92 and Leu14, in *Ph. laminosum* Pc (*10*). This implies, at least for these crucial residues, that the mode of interaction and the resulting change in chemical environment is similar in both complexes.

DISCUSSION

NMR titration curves reveal that *P. hollandica* Pc and *Ph. laminosum* cyt*f* form a complex of 1:1 stoichiometry with a binding affinity of 6 (±2) × 10^3 M^{-1}, about 20-fold higher than that of the physiological Pc (Figure 6). Chemical-shift perturbation mapping implies that the hydrophobic patch of Pc dominates the complex interface (Figure 8). This suggests that *P. hollandica* Pc utilizes a "head-on" interaction to maximize hydrophobic contacts with cyt*f*, similar to the

complex formed between *Ph. laminosum* Pc and cyt*f* (Figure 1) (*10*). It is a surprising result that the binding affinity of the native complex between *Ph. laminosum* Pc and cyt*f* is 1 order of magnitude lower than observed with the nonphysiological *P. hollandica* Pc. Although the complex interface is composed of the hydrophobic patch, variations in the electrostatic features of the two Pc molecules must contribute to the difference in binding affinity. Both Pc and cyt*f* from *Ph. laminosum* are acidic proteins with p*I* values < 5. In contrast, Pc from *P. hollandica* is a basic protein (p*I* > 8), which enables attractive electrostatic interactions with the acidic cyt*f*. Apart from the difference in p*I*, the arrangement of lysines is also important. Five of the six Lys residues found in *P. hollandica* Pc are intimately associated with the binding site and experience a significant $\Delta\delta_{Avg}$ in the complex with cyt*f* (Figure 8). In contrast, only the two conserved lysines, Lys6 and Lys35, are located near the binding site in *Ph. laminosum* Pc. Presumably the juxtaposition of lysines and the hydrophobic patch in *P. hollandica* Pc renders the protein capable of forming a tighter complex with cyt*f*. This idea is supported by the observation that the complex with *P. hollandica* Pc is susceptible to ionic strength effects (Figure 9) while the complex formed with *Ph. laminosum* Pc is unaffected by salt (*10*).

On the basis of the $^1H^N$ resonance assignments, it can be concluded that the structure of the hydrophobic patch in *P. hollandica* Pc resembles that of *Ph. laminosum* Pc. The double mutation Y12G/P14L produces a protein with a greater resemblance to *Ph. laminosum* Pc. A difference plot of the resonance assignments for *P. hollandica* Pc and Pc Y12G/P14L highlights the residues, which are affected by the mutations (Figure 2). The affected region corresponds to the four loops in the north end of the protein, which are also involved in complex formation with cyt*f* (Figure 7). Despite the steric alterations introduced into the binding site of *P. hollandica* Pc, the affinity for cyt*f* was not affected by the Y12G/P14L mutations. A comparable situation has been reported for the interactions of Pc and PSI from *P. hollandica* (*27*). It was found that the binding constant for complex formation between PSI and Pc ($\sim 10^4$ M^{-1}) was not significantly influenced by the mutation of either Tyr12 or Pro14.

Considering that the atoms in protein−protein interfaces are close-packed (*41*), it is surprising that *P. hollandica* Pc and Pc Y12G/P14L have such similar affinities for cyt*f*. The similar binding affinity may indicate that surface complementarity is of less importance in transient complex formation. This could be a necessary feature in order (i) not to jeopardize the required low affinity and (ii) to facilitate interactions between proteins, which have more than one partner. This suggestion is supported by the fact that transient complexes are readily formed between nonphysiological partners (*42*). Furthermore, the results of mutagenesis studies on the interactions of plant Pc suggest that the structure of the hydrophobic patch is a compromise between optimal binding to cyt*f* and PSI. It has been demonstrated that the introduction of a bulky residue in place of Gly10 reduces the efficiency of electron transfer to PSI (*21*), yet increases the electron-transfer rate for reduction by cyt*bf* particles (*20*).

Although the binding affinity for cyt*f* was unaffected by the mutations, the appearance of the chemical-shift map was altered both qualitatively and quantitatively (Figures 7 and 8). To compare the chemical-shift perturbation in both complexes, the shifts were extrapolated to 100% bound ($\Delta\delta_{Max}$), and $\Delta\delta_{Avg}$ was calculated for each backbone amide. Only 12 residues (including Gly37, His39, Asn40, Cys82, and His85) have a $\Delta\delta_{Avg}$ that is within 80% similar in both complexes. The most conspicuous difference between the complexes is that $\Delta\delta_{Avg}$ is on average 40% decreased for the double mutant (Figure 7). Large chemical-shift changes were observed for residues 10−15 upon mutation of Y12G/P14L (Figure 2). Three of these residues (Tyr12, Ala13, Leu15) demonstrate the largest shifts in *P. hollandica* Pc upon complex formation (Figure 7A). Therefore, it is plausible that the large shifts in the complex report on changes occurring around Tyr12. For example, Tyr12 may undergo a conformational change to accommodate the binding site on cyt*f*, thus triggering the large shifts for the neighboring residues. This would not account for the clear difference in the binding maps, around residues Leu60, Ala63, Thr83, and Arg86 (Figures 7 and 8). These residues were not significantly affected by the mutations (Figure 2). Perhaps, however, the binding orientation of the mutant is altered with respect to the wild-type protein, causing global differences in the chemical-shift maps.

An alternative explanation for the overall reduction in Δ_{Avg} is an increase in the dynamics of the mutant complex. While one orientation may be optimal in terms of geometric fitting, there can exist a cluster of conformations around the optimum, which do not differ significantly in energy. In the case of the wild-type Pc, the presence of Tyr12 reduces the number of possible conformations by steric hindrance. In Pc Y12G/P14L, the flatter surface can explore a greater number of orientations and the chemical-shift changes are averaged out. This hypothesis is supported by the fact that the line broadening effects, arising from complex formation, were decreased in the mutant complex compared with the wild-type complex. The less extensive binding site of Pc Y12G/P14L (Figure 8) is also in agreement with conformational averaging. Those residues on the periphery of the interface, which experience small shifts in *P. hollandica* Pc, are consequently below the cutoff (<0.025 ppm) in the complex with Pc Y12G/P14L.

An extreme form of such conformational averaging (with a 20-fold decrease in $\Delta\delta_{Max}$) has been observed in the complexes of Pc and cytochrome *c* (*43*) and cytochrome b_5 and myoglobin (*44*). Rather than adopting a single orientation, these complexes consist of a dynamic ensemble involving multiple binding sites, dominated by electrostatic interactions (*43*-*46*). In the complex of Pc and cyt*f*, the dynamics are more limited, as hydrophobic interactions ensure the formation of a relatively well-defined complex. The double mutation in *P. hollandica* Pc (Y12G/P14L) appears to shift the balance in the Pc-cyt*f* complex toward increased dynamics.

ACKNOWLEDGMENT

P.B.C. gratefully acknowledges R.E.M. Diederix for helpful discussions and C. Erkelens for assistance with the NMR facilities.

SUPPORTING INFORMATION AVAILABLE

Table of all residues which experienced a $|\Delta\delta_{Bind}| \geq 0.02$ ($^1H^N$) or ≥ 0.10 (^{15}N) in the complexes of cyt*f* with *P.*

hollandica Pc and Pc Y12G/P14L. This material is available free of charge via the Internet at http://pubs.acs.org.

REFERENCES

1. Mitchell, P. (1976) *J. Theor. Biol. 62*, 327−367.
2. Bendall, D. S. (1996) in *Protein Electron Transfer* (Bendall, D. S., Ed.) pp 43−68, Bios Scientific, Oxford.
3. McLendon, G. (1991) *Struct. Bond. 75*, 159−174.
4. Williams, P. A., Fulop, V., Leung, Y. C., Chan, C., Moir, J. W. B., Howlett, G., Ferguson, S. J., Radford, S. E., and Hajdu, J. (1995) *Nat. Struct. Biol. 2*, 975−982.
5. Gross, E. L. (1996) in *Oxygenic Photosynthesis: The Light Reactions* (Ort, D. R., and Yocum, C. F., Eds.) pp 413−429, Kluwer Academic Publishers, Dordrecht, The Netherlands.
6. Sigfridsson, K. (1998) *Photosynth. Res. 57*, 1−28.
7. Gray, J. C., Rochford, R. J., and Packman, L. C. (1994) *Eur J. Biochem. 223*, 481−488.
8. Martinez, S. E., Huang, D., Szczepaniak, A., Cramer, W. A., and Smith, J. L. (1994) *Structure 2*, 95−105.
9. Ubbink, M., Ejdeback, M., Karlsson, B. G., and Bendall, D. S. (1998) *Structure 6*, 323−335.
10. Crowley, P. B., Otting, G., Schlarb-Ridley, B. G., Canters, G. W., and Ubbink, M. (2001) *J. Am. Chem. Soc. 123*, 10444−10453.
11. Kannt, A., Young, S., and Bendall, D. S. (1996) *BBA-Bioenergetics 1277*, 115−126.
12. Hope, A. B. (2000) *BBA-Bioenergetics 1456*, 5−26.
13. Schlarb-Ridley, B. G., Bendall, D. S., and Howe, C. J. (2002) *Biochemistry 41*, 3279−3285.
14. Colman, P. M., Freeman, H. C., Guss, J. M., Murata, M., Norris, V. A., Ramshaw, J. A. M., and Venkatappa M. P. (1978) *Nature (London) 272*, 319−324.
15. Guss, J. M., and Freeman, H. C. (1983) *J. Mol. Biol. 169*, 521−563.
16. Thompson, J. D., Plewniak, F., Thierry, J.-C. and Poch, O. (2000) *Nucleic Acids Res. 28*, 2919−2926.
17. Kohzuma, T., Inoue, T., Yoshizaki, F., Sasakawa, Y., Onodera, K., Nagatomo, S., Kitagawa, T., Uzawa, S., Isobe, Y., Sugimura, Y., Gotowda, M., and Kai, Y. (1999) *J. Biol. Chem. 274*, 11817−11823.
18. De Rienzo, F., Gabdoulline, R. R., Menziani, M. C., and Wade, R. C. (2000) *Protein Sci. 9*, 1439−1454.
19. Modi, S., Nordling, M., Lundberg, L. G., Hansson, O., and Bendall, D. S. (1992) *Biochim. Biophys. Acta 1102*, 85−90.
20. Illerhaus, J., Altschmied, L., Reichert, J., Zak, E., Herrmann, R. G., and Haehnel, W. (2000) *J. Biol. Chem. 275*, 17590−17595.
21. Haehnel, W., Jansen, T., Gause, K., Klosgen, R. B., Stahl, B., Michl, D., Huvermann, B., Karas M., and Herrmann, R. G. (1994) *EMBO J. 13*, 1028−1038.
22. Sigfridsson, K., Young, S., and Hansson, Ö. (1996) *Biochemistry 35*, 1249−1257.
23. Babu, C. R., Arudchandran, A., Hille, R., Gross, E. L., and Bullerjahn, G. S. (1997) *Biochem. Biophys. Res. Commun. 235*, 631−635.
24. Babu, C. R., Volkman, B. F., and Bullerjahn, G. S. (1999) *Biochemistry 38*, 4988−4995.
25. Schlarb, B. G., Wagner, M. J., Vijgenboom, E., Ubbink, M., Bendall, D. S., and Howe, C. J. (1999) *Gene 234*, 275−283.
26. Sambrook, J., Fritsch, E. F., and Maniatis, T. (1989) *Molecular Cloning: A Laboratory Manual*, 2nd ed., Cold Spring Harbor Laboratory, Cold Spring Harbor, NY.
27. Navarro, J. A., Myshkin, E., De la Rosa, M. A., Bullerjahn, G. S., and Hervás, M. (2001) *J. Biol. Chem. 276*, 37501−37505.
28. Andersson, P., Weigelt, J., and Otting, G. (1998) *J. Biomol. NMR 12*, 435−441.
29. Bartels, Ch., Xia, T.-H., Billeter, M., Güntert P., and Wüthrich, K. (1995) *J. Biomol. NMR 5*, 1−10.
30. Grzesiek, S., Bax, A., Clore, G. M., Gronenborn, A. M., Hu, J.-S., Kaufman, J., Palmer, I., Stahl, S. J., and Wingfield, P. T. (1996) *Nat. Struct. Biol. 3*, 340−345.
31. Nicholls, A., Sharp, K., and Honig, B. (1991) *Prot. Struct. Funct. Genet. 11*, 281−96.
32. Guex, N., and Peitsch, M. C. (1997) *Electrophoresis 18*, 2714−2723.
33. Potts, B. C. M., and Chazin, W. J. (1998) *J. Biomol. NMR 11*, 45−57.
34. Segal, M. G., and Sykes, A. G. (1978) *J. Am. Chem. Soc. 100*, 4585−4592.
35. Kojiro, C. L., and Markley, J. L. (1983) *FEBS Lett. 162*, 52−56.
36. Guss, J. M., Harrowell, P. R., Murata, M., Norris, V. A., and Freeman, H. C. (1986) *J. Mol. Biol. 192*, 361−387.
37. Hunter, D. M., McFarlane, W., Sykes, A. G., and Dennison, C. (2001) *Inorg. Chem. 40*, 354−360.
38. Dennison, C., Lawler, A. T., and Kohzuma, T., (2002) *Biochemistry 41*, 552−560.
39. P. B. Crowley (2002) *Transient Protein Interactions of Photosynthetic Redox Partners*, Ph.D. Thesis, Leiden University, Leiden, The Netherlands.
40. Zuiderweg, E. R. P. (2002) *Biochemistry 41*, 1−7.
41. Lo Conte, L., Chothia, C., and Janin, J. (1999) *J. Mol. Biol. 285*, 2177−2198.
42. Crowley, P. B., Rabe, K. S., Worrall, J. A. R., Canters, G. W., and Ubbink, M. (2002) *ChemBioChem 3*, 526−533.
43. Ubbink, M., and Bendall, D. S. (1997) *Biochemistry 36*, 6326−6335.
44. Worrall, J. A. R., Liu, Y., Crowley, P. B., Nocek, J. M., Hoffman, B. M., and Ubbink, M. (2002) *Biochemistry 41*, 11721−11730.
45. Furukawa, Y., Matsuda, F., Ishimori, K., and Morishima, I. (2002) *J. Am. Chem. Soc. 124*, 4008−4019.
46. Liang, Z. X., Nocek, J. M., Huang, K., Hayes, R. T., Kurnikov, I. V., Beratan, D. N., and Hoffman, B. M. (2002) *J. Am. Chem. Soc. 124*, 6849−6859.
47. Bond, C. S., Bendall, D. S., Freeman, H. C., Guss, J. M., Howe, C. J., Wagner, M. J., and Wilce, M. C. J. (1999) *Acta Crytallogr., Sect. D 55*, 414−421.
48. Carrell, C. J., Schlarb, B. G., Bendall, D. S., Howe, C. J., Cramer, W. A., and Smith, J. L. (1999) *Biochemistry 38*, 9590−9599.
49. Kraulis, P. J. (1991) *J. Appl. Crystallogr. 24*, 946−950.
50. Merritt, E. A., and Bacon, D. J. (1997) *Methods Enzymol. 277*, 505−524.

BI026349B